University of Glasgow

VIA VERITAS VITA

Gandhi, N., Jaisawal, R. K., Rathore, S., Kondekar, P. N., Dixit, A., Kumar, N. , Georgiev, V. and Bagga, N. (2023) Gate Oxide Induced Reliability Assessment of Junctionless FinFET-Based Hydrogen Gas Sensor. In: 2023 IEEE SENSORS, Vienna, Austria, 29 Oct - 01 Nov 2023, ISBN 9798350303872 (doi: 10.1109/SENSORS56945.2023.10324885)

Copyright © 2023 IEEE. Personal use of this material is permitted. Permission from IEEE must be obtained for all other uses, in any current or future media, including reprinting/republishing this material for advertising or promotional purposes, creating new collective works, for resale or redistribution to servers or lists, or reuse of any copyrighted component of this work in other works.

This is the author version of the work. There may be differences between this version and the published version. You are advised to consult the published version if you wish to cite from it:
https://doi.org/10.1109/SENSORS56945.2023.10324885

https://eprints.gla.ac.uk/310981/

Deposited on 05 January 2024

Enlighten – Research publications by members of the University of Glasgow
http://eprints.gla.ac.uk

Gate Oxide Induced Reliability Assessment of Junctionless FinFET-based Hydrogen Gas Sensor

Navneet Gandhi[1], Rajeewa Kumar Jaisawal[1], Sunil Rathore[1], P. N. Kondekar[1], Ankit Dixit[2], Navneen Kumar[2] Vihar Georgiev[2], and Navjeet Bagga[3]

[1]VLSI Lab, Electronics & Communication Department, PDPM- IIITDM, Jabalpur, India, [2]University of Glasgow, United Kingdom, [3]School of Electrical Sciences, Indian Institute of Technology Bhubaneswar, India. (Corresponding Author Email: navjeet@iitbbs.ac.in).

***Abstract*—Gate oxide plays a crucial role in the performance of nano-scaled emerging devices. In FET-based sensors, gate-oxide-induced reliability analysis is essential for credible sensing. In this paper, using well-calibrated TCAD models, we analyzed the role of gate-induced drain leakage (GIDL) in a Junctionless FinFET-based Hydrogen (H_2) gas sensor. Owing to high diffusivity and solubility, the Palladium (Pd) metal is employed as the gas-sensing surface, where the absorbed H_2 molecules modulate the effective work function and, in turn, the threshold voltage (V_{th}), opted as primary sensing merit. In a Junctionless device, the heavily doped and fully depleted channel leads to significant band overlapping between the channel and drain regions, in turn, causes band-to-band tunneling. Therefore, a proper design guideline that governs the effective channel conduction modulation is worth needed for the reliable operation of an H_2 sensor.**

Keywords—GIDL; Adsorption; BTBT; DIBL; Parasitic bipolar transistor; Pressure, Temperature.

I. Introduction

FinFET-based CMOS devices are in volume production due to ultra-low power levels usability, fabrication compatibility, reduced short channel effect (SCE), better gate electrostatic controllability, and improved switching response compared to the conventional MOSFET [1]-[2]. However, the abrupt doping profile in the source/drain-channel junction demands a costly/complex annealing process to overcome the overlap capacitance and series resistance [3]-[4]. Thus, Junctionless field-effect transistors (JL-FETs) offer a solution to the challenges associated with the conventional flow by eliminating the need for a pn-junction, employing a uniform doping profile throughout the channel region, and featuring a simplified fabrication process [5]-[6]. Following the research trend, the Junctionless FinFET employed as a hydrogen gas sensor combines the strengths of Junctionless and FinFET technologies integrated with a catalytic metal gate (Pd), which plays a crucial role in detecting H_2 gas molecules by monitoring changes in the gate's work function [7]-[12]. The choice of Pd as the catalytic gate metal is deliberate, as it exhibits high diffusivity and solubility by absorbing H_2 from the external environment onto the metal gate, resulting in enhanced sensing merits [7]-[9], [13]-[14]. The hydrogen molecules dissociate into atomic hydrogen, dissolving in the metal and diffusing towards the metal-oxide interface. At the interface, the presence of atomic hydrogen induces the formation of a dipole layer [10]. This dipole layer alters the work-function difference between the metal and the semiconductor, leading to a change in the threshold voltage of the proposed gas sensor. Henceforth, the change in threshold voltage can be easily measured electrically, providing a means for detecting the concentration of hydrogen gas [15]. Despite the advantages, Junctionless FinFET comprises an ultra-thin and heavily-doped semiconductor layer, volume-depleted due to a large work function difference. This leads to band overlapping between the channel's valence band and the drain's conduction band. Moreover, drain-induced barrier lowering (DIBL) introduces the leakage component. Therefore, a significantly large leakage current flows owing to GIDL & DIBL [16], which severely influences the reliability of the proposed H_2 sensor. Thus, through an extensive TCAD study, we analyzed: (*i*) the impact of GIDL and DIBL in the proposed JL-FinFET-based H_2 sensor; (*ii*) the electrical characteristics of the sensor at different gas concentrations (in ppm); (*iii*) the performance comparison with varying doping concentration and fin thicknesses, and without considering the GIDL models in TCAD.

II. Device structure and simulation setup

Fig.1(a) depicts a three-dimensional schematic view of the baseline Junctionless FinFET, considered for realizing a JL-FinFET-based H_2 sensor (Fig.1c). The Pd catalysis metal is used in the proposed sensor as an active sensing surface. The JL-FinFET consists of a silicon fin with uniform n-type doping in the source, channel, and drain regions to minimize series resistance, overlap capacitance, and random dopant fluctuation (RDF). Table-I provides the specific device dimensions used in the simulation, considered the default values unless stated otherwise. The gate region is stacked with Palladium (Pd) metal as the gas sensing element and a stacked oxide with effective oxide thickness (EOT) of 1nm.

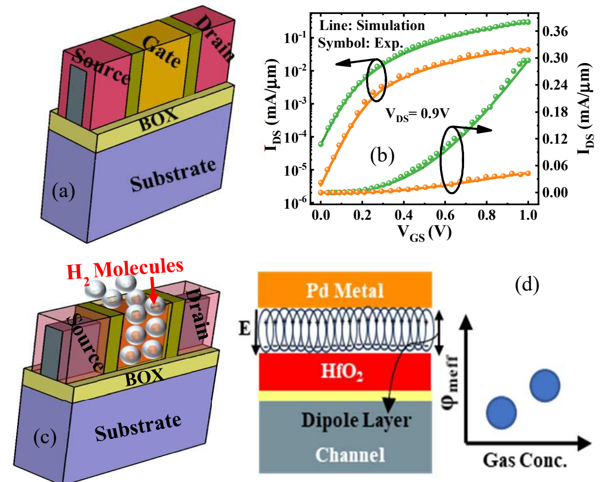

Fig. 1: (a) schematic of the baseline Junctionless FinFET; (b) TCAD calibration against the experimental data of the baseline device [17]; (c) schematic of realized JL-FinFET based H_2 sensor; (d) demonstration of minuscule level interaction of H_2 gas with Pd metal gate, which forms the dipole layer and ultimately varies the effective work function.

Table-I: DEVICE PARAMETERS

Parameter	Value
Channel length (Lg)	30nm
Channel/source/drain Doping (N_D)	$2\times10^{19}cm^{-3}$
Pd Metal Work Function	5.2eV
Source/drain Metal Work Function	5.2eV
Substrate Thickness	50nm
Buried Oxide (BOX) Thickness	10nm
Height of the fin (H_{Fin})	29nm
Fin thickness (T_{Fin})	10nm

The TCAD models are well-calibrated against the experimental data [17], as shown in Fig. 1(b). The conventional drift-diffusion model is employed for carrier transport. The Philips unified mobility model governs the impurity scattering and mobility variations in the heavily doped silicon fin (channel). The Lombardi and Grad quasi-fermi models are also considered for surface roughness, acoustic surface phonons, and electric field induce mobility degradation, respectively. The bandgap narrowing effect is incorporated using the Old Slotboom model. The carrier generation and recombination processes are assessed using the SRH and Auger models.

A. H_2 Gas Sensing Methodology:

Fig. 1(d) briefly shows the sensing methodology and how gas concentration modulates the metal work function, in turn, the sensing merit (i.e., especially to V_{th}). Hydrogen is a colorless, tasteless, and odorless gas that poses safety risks due to its high combustion rates and rapid burning velocity, necessitating prompt leak detection. Under normal conditions, hydrogen gas consists of diatomic molecules comprising two hydrogen atoms bonded through covalent interactions. During the transduction mechanism, the process involves the dissociation and adsorption of hydrogen molecules on the surface of a palladium metal gate. The variation in the metal gate work function with the concentration of the hydrogen gas is given as

$$\Delta\emptyset_m = M_q - \left[\left(\frac{RT}{4F}\right) * In(P)\right] \quad (1)$$

Here, R=8.314 $JM^{-1}K^{-1}$ is the gas constant, T=300K is ambient temperature, F=96500CM^{-1} is Faraday's constant, and P= 2.5Pa is the partial pressure of gas [15]. Thus, the effective metal gate work function after the diffusion of hydrogen gas molecules is

$$\emptyset_{meff} = \emptyset_m \pm \Delta\emptyset_m \quad (2)$$

φ_m is the metal work function of the baseline device.

For the limiting reaction of the model, if we assume that all hydrogen atom at the adsorption site of metal surface reached at the interface adsorption site (A_{Int}). Then

$$A_{Int} = H_{Surf} \quad (3)$$

For X concentration (in ppm) of the hydrogen gas, the equivalent value is 0.001*X gm/l, where dividing gm/l by the molecular mass of hydrogen (i.e., 2.016gm/mol) gives the molar concentration of hydrogen (M/l) for X ppm. Table II gives the surface concentration value for different gas concentrations varying from 1.0 ppm to 2.0 ppm. The equivalent surface charge (M_q) is given by:

$$M_q = 0.001\times H_{Surf} \quad (4)$$

Table II: SURFACE CONCENTRATION OF H2 AT DIFFERENT GAS CONCENTRATION

Conc. (ppm)	Conc. (gm/l)	Molar Conc.= Conc./Molecular mass (M/l)	$H_{Surf}=q_H\times$molar Conc.$\times$ Avogadro no. (charge per cm^3)
1.0	0.001	4.96×10^{-4}	5.9748×10^{20}
1.5	0.0015	7.44×10^{-4}	9.2702×10^{20}
2.0	0.002	9.92×10^{-4}	1.1949×10^{21}
q_H =No. of atoms/proton charge =2			

III. RESULT AND DISCUSSION

The gas molecules adsorbed on the surface of a catalytic metal gate (Palladium) induce work function modulation, consequently altering the electrical parameters of the device. Using the above hydrogen sensing methodology, we can calculate the electrical performance and sensitivity of proposed gas sensor at different gas concentrations.

$$S_A(\%) = \frac{(A=0ppm)-(A>0ppm)}{(A=0ppm)} \times 100 \quad (5)$$

Here, A represents various electrical parameters like threshold voltage (V_{th}), ON current (I_{ON}), OFF current (I_{OFF}), etc., of the proposed gas sensor at different ppm values.

A. Electrical Performance and Sensitivity Analysis

The transfer characteristic (I_{DS}-V_{GS}) of the proposed JL-FinFET-based hydrogen sensor at different ppm values is shown in Fig.2(a). The increases in hydrogen gas concentration at the surface of the Pd metal gate result in the formation of a dipole layer at the metal-oxide interface, in turn, causes an induced internal electric field. This internal electric field decreases the surface potential; therefore, a higher gate voltage is required to accumulate the channel charges. Thus, the threshold voltage and, in turn, the ON current of the device changes, as shown in the inset of Fig.2(a), with varying H_2 gas concentrations. Fig.2(b) shows the corresponding sensitivity of the sensor in terms of V_{th} and I_{ON}. The observed maximum V_{th} sensitivity is 82.56% for 2.0ppm H_2 gas concentration and experimentally

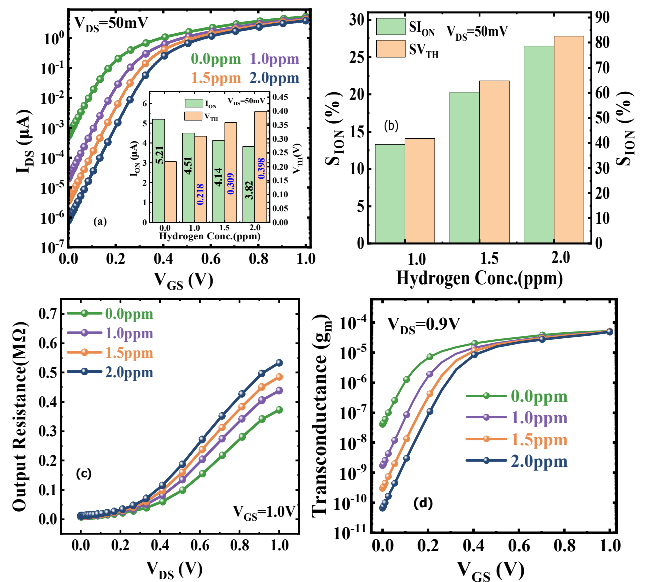

Fig.2 Impact of varying hydrogen gas concentration from 1.0 ppm to 2.0 ppm on (a) I_{DS}-V_{GS} characteristic (inset shows the threshold voltage and ON current variation); (b) threshold voltage and ON current sensitivity; (c) output resistance; and (d) transconductance (g_m) of the proposed JL-FinFET.

observed response is ~23.59% for 1.0ppm of H_2 gas [3]. The internally formed dipole layer increases the vertical electric field by increasing the H_2 concentration and, in turn, severely affects carrier mobility. Thus, alters the I_{ON} sensitivity. Further, the transconductance (g_m) and output resistance of the FinFET are key electrical parameters that can be used as sensing metrics (Fig.2c-d). The value of g_m exhibits a negative correlation with increasing H_2 concentration (Fig.2d). This can be attributed to the rise in the internal electric field resulting from the higher concentration. Additionally, the mobility of the device experiences a decline as concentration increases.

B. Role of GIDL on Sensing Performance

This section examines the impact of GIDL current resulting from band-to-band tunneling (BTBT) between the channel valence band and the drain conduction band. To incorporate BTBT, the nonlocal tunneling model is included in the TCAD setup. Fig.3 shows a contour plot of a JL-FinFET, showing a significant accumulation of hole concentration during electron tunneling from the channel to the drain region. Fig.4 (a) represents the lateral band diagram of JL-FinFET at a different gate voltage. A significant band overlapping occurred at gate voltage less than zero volts. The minimum tunneling width measured at V_{GS}=0V is approximately 6nm. Fig.4 (b) represented the band diagram at gate voltage ‘0 V’ for different ppm values when BTBT tunneling occurred. Increasing the hydrogen concentration increases the band gap separation, which increases the device's threshold voltage. The elevated threshold voltage effectively reduces the off-state leakage current of the device. Fig.4(c) represents the I_{DS}-V_{GS} characteristic for different hydrogen gas concentrations, and in Fig.4(d), the band diagram is presented at 0 ppm for different drain voltages while maintaining a gate voltage of 0.0V. The drain-induced barrier lowering (DIBL) effect significantly decreases the source-side potential as the drain voltage increases. Therefore, GIDL and DIBL profoundly impacted the sensing performance.

C. Dimensional Variation on the Sensor Performance

In Fig.5(a), the I_{DS}-V_{GS} characteristic is depicted for three different fin thicknesses: 10nm, 8nm, and 6nm, at a constant drain voltage of 0.9V, under the condition of 0.0ppm. As fin thickness decreases, the device's threshold voltage exhibits an augmented value compared to a thicker fin layer. Consequently, this increment in threshold voltage engenders a decrease in the I_{OFF} of the device. Furthermore, it is worth noting that the DIBL effect is more pronounced at the source-drain edge in thick fin layers compared to thin fin layers. This leads to a decrease in the threshold voltage and an increase in the I_{OFF} for thick fin layers. The variation in the band diagram at different fin thicknesses is depicted in Fig.5(b). Further, with an increase in the concentration of hydrogen gas, the influence of DIBL starts to decrease (in %) at each specific fin thickness. impact of varying channel doping from: $2\times10^{19}/cm^3$, $1\times10^{19}/cm^3$, and $6\times10^{18}/cm^3$ for 0.0ppm shown in Fig.5(c). It is observed that the GIDL current decreases to some extent as the internal electric field diminishes due to low channel doping. The effect of doping on the band structure of JL-FinFET at 0.0ppm is shown in Fig.5(d).

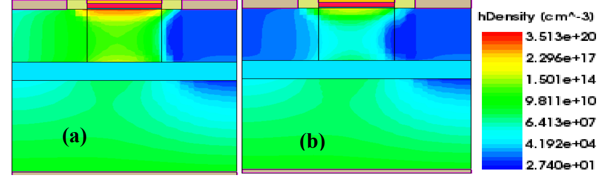

Fig. 3: Contour plot representation of JL-FinFET-based H_2 sensor (a) when BTBT is considered and (b) when BTBT is not considered, for the V_{GS}= 0.0V, T_{Fin}=10nm, and absence of hydrogen gas (0.0 ppm).

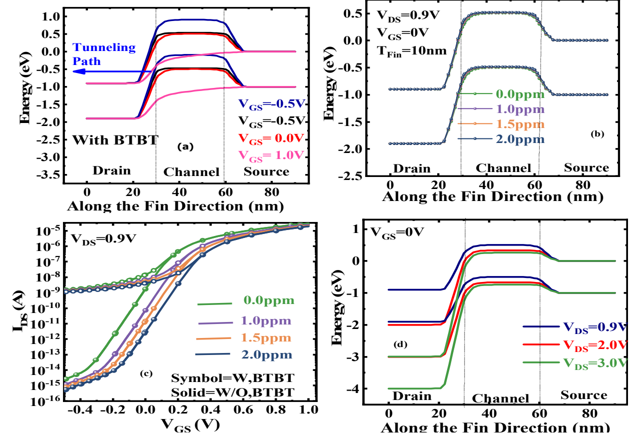

Fig.4: Impact of BTBT tunneling on (a) lateral band diagram at different gate voltage for 0.0 ppm value; (b) band diagram at different hydrogen concentrations for V_{GS}= 0V; (c) I_{DS}-V_{GS} characteristics at different ppm value with and without BTBT; and (d) effect of DIBL on energy band diagram at various drain voltage for 0.0 ppm value.

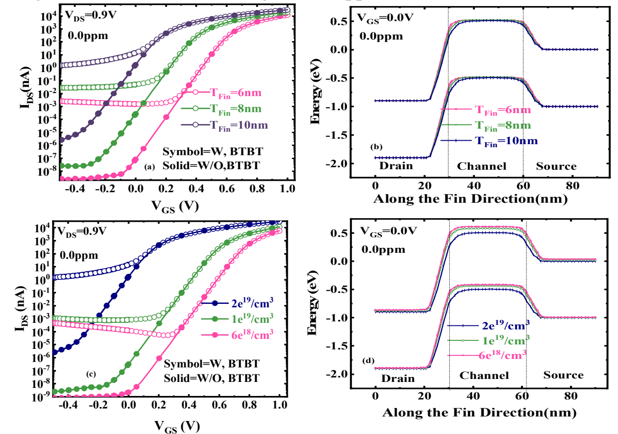

Fig.5: Impact of varying the Fin thickness and channel doping concentration on (a,c) transfer characteristics and (b,d) energy band diagram of the JL-FinFET-based H_2 sensor at 0.0ppm.

IV. CONCLUSION

Using well-calibrated TCAD models, we comprehensively investigated the electrical performance of the proposed Junctionless FinFET-based hydrogen gas sensor at different H_2/air concentrations. We opted to analyze the threshold voltage (V_{th}) as a prime sensing parameter. The sensitivity in terms of ON current and V_{th} is calculated for varying H_2 concentrations, which shows that higher concentration increases the channel conduction. Further, the effect of gate oxide-induced GIDL and drain voltage-induced DIBL is investigated in sensor performance, followed by varying channel doping and fin thickness is investigated. The proposed guideline suggests that the proposed Junctionless FinFET possessing a thicker fin and exposed at low hydrogen concentration is more susceptible to the GIDL effect.

REFERENCES

[1]. S. Kaushal and A. K. Rana, "Negative Capacitance Junctionless FinFET for Low Power Applications: An Innovative Approach," Silicon, Oct.2021, doi: 10.1007/s12633-021-01392-x.

[2]. R. K. Jaisawal, S. Rathore, P. N. Kondekar and N. Bagga, "Analog/RF and Linearity Performance Assessment of a Negative Capacitance FinFET using High Threshold Voltage Techniques," in IEEE Transactions on Nanotechnology, doi: 10.1109/TNANO.2023.3308814.

[3]. N. Gandhi, S. Rathore, R. K. Jaisawal, P. N. Kondekar, S. Dey, and N. Bagga, "Unveiling the Self-Heating and Process Variation Reliability of a Junctionless FinFET-based Hydrogen Gas Senso," IEEE Sensors Letters, doi: 10.1109/LSENS.2023.3309263.

[4]. S. Sahay and M. Jagadesh Kumar, "Junctionless Field-Effect Transistors: Design, Modeling, and Simulation," Junctionless Field-Effect Transistors Des. Model. Simul., pp. 1–457, Jan. 2019, doi: 10.1002/9781119523543

[5]. K. Tsukada *et al.*, "Dual-Gate field-effect transistor hydrogen gas sensor with thermal compensation," *Jpn. J. Appl. Phys.*, vol. 49, no. 2 Part 1, Nov. 2010, doi: 10.1143/JJAP.49.024206.

[6]. K. Scharnagl, A. Karthigeyan, M. Burgmair, M. Zimmer, T. Doll, and I. Eisele, "Low-temperature hydrogen detection at high concentrations: Comparison of platinum and iridium," *Sensors Actuators, B Chem.*, vol. 80, no. 3, pp. 163–168, Dec. 2001, doi: 10.1016/S0924-4247(01)006720.

[7]. D. Sarkar, H. Gossner, W. Hansch, and K. Banerjee, "Tunnel-field-effect-transistor based gas-sensor: Introducing gas detection with a quantum-mechanical transducer," *Appl. Phys. Lett.*, vol. 102, no. 2, Jan. 2013, doi: 10.1063/1.4775358.

[8]. I. Lundström, S. Shivaraman, C. Svensson, and L. Lundkvist, "A hydrogen-sensitive MOS field-effect transistor," *Appl. Phys. Lett.*, vol. 26, no. 2, pp. 55–57, 1975, doi: 10.1063/1.88053.

[9]. S. Mokkapati, N. Jaiswal, M. Gupta, and A. Kranti, "Gate-All-Around Nanowire Junctionless Transistor-Based Hydrogen Gas Sensor," *IEEE Sens. J.*, vol. 19, no. 13, pp. 4758–4764, Mar. 2019, doi: 10.1109/JSEN.2019.2903216.

[10]. L.-G. Ekedahl, M. Eriksson, and I. Lundström, "Hydrogen Sensing Mechanisms of Metal−Insulator Interfaces," *Acc. Chem. Res.*, vol. 31, no. 5, pp. 249–256, May 1998, doi: 10.1021/ar970068s.

[11]. K. M. Choi and W. Y. Choi, "Work-function variation effects of tunneling field-effect transistors (TFETs)," *IEEE Electron Device Lett.*, vol. 34, no. 8, pp. 942–944, Jun. 2013, doi: 10.1109/LED.2013.2264824.

[12]. S. Rathore, R. K. Jaisawal, P. N. Kondekar and N. Bagga, "Demonstration of a Nanosheet FET With High Thermal Conductivity Material as Buried Oxide: Mitigation of Self-Heating Effect," in IEEE Transactions on Electron Devices, vol. 70, no. 4, pp. 1970-1976, April 2023, doi: 10.1109/TED.2023.3241884.

[13]. R. Gautam, M. Saxena, R. S. Gupta, and M. Gupta, "Gate-all-around nanowire MOSFET with catalytic metal gate for gas sensing applications," *IEEE Trans. Nanotechnol.*, vol. 12, no. 6, pp. 939–944, Aug. 2013, doi: 10.1109/TNANO.2013.2276394.

[14]. H. D. Sehgal, Y. Pratap, M. Gupta, and S. Kabra, "Performance investigation of novel Pt/Pd-SiO2Junctionless FinFET as a high sensitive hydrogen gas sensor for industrial applications," *IEEE Sens. J.*, vol. 21, no. 12, pp. 13356–13363, Mar. 2021, doi: 10.1109/JSEN.2021.3067801

[15]. A. Varghese, A. Eblabla, and K. Elgaid, "Modeling and Simulation of Ultrahigh Sensitive AlGaN/AlN/GaN HEMT-Based Hydrogen Gas Detector with Low Detection Limit," *IEEE Sens. J.*, vol. 21, no. 13, pp. 15361–15368, Jul. 2021, doi: 10.1109/JSEN.2021.3072476.

[16]. S. Parke, J. Moon, H. Wann, P. Ko, and C. Hu, "Design for suppression of gate-induced drain leakage in LDD MOSFETs using a quasi-two-dimensional analytical model," IEEE Trans. Electron Devices, vol. 39, no. 7, pp. 1694–1703, Jul. 1992.

[17]. R. Rios *et al.*, "Comparison of junctionless and conventional trigate transistors with L g down to 26 nm," *IEEE Electron Device Lett.*, vol. 32, no. 9, pp. 1170–1172, Jul. 2011, doi: 10.1109/LED.2011.2158978.